HIDDEN DEGREES OF FREEDOM

Nucleons

proton:

$$uud$$

$$uud(u\bar{u})$$

$$uud(d\bar{d})$$

Hidden strangeness:

$$uud(s\bar{s})$$

4 experiments: SAMPLE, HAPPEX, A4, G0

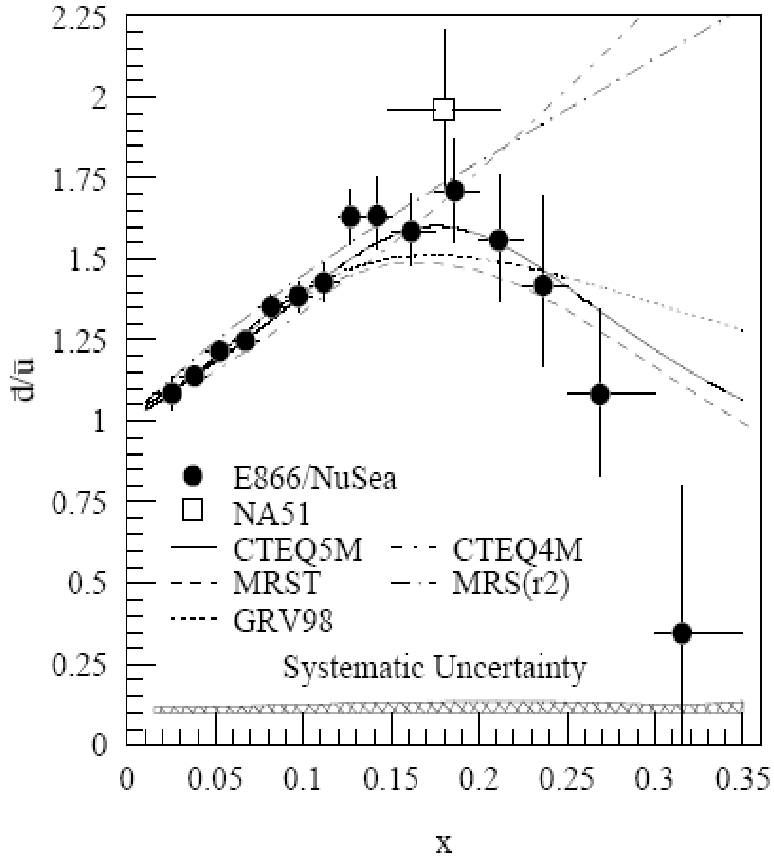

Figure 6: The ratio of $\bar{d}/\bar{u}$ in the proton as a function of x extracted from the Fermilab E866 cross section ratio. The curves are parametrizations of various parton distribution functions. The error bars indicate statistical errors only. Also shown is the result from NA51, plotted as an open box.

G.Garvey and J.C.Peng, Prog.Part.Nucl.Phys. 47, 203 (2001)

$$\boxed{s\bar{s}\ \text{COMPONENT}}$$

PARITY VIOLATING ELECTRON SCATTERING

QUARK CURRENTS

$$V_\mu^\gamma = \frac{2}{3}\bar{u}\gamma_\mu u - \frac{1}{3}\bar{d}\gamma_\mu d - \frac{1}{3}\bar{s}\gamma_\mu s$$

$$V_\mu^Z = \left(1-\frac{8}{3}s\right)\bar{u}\gamma_\mu u + \left(-1+\frac{4}{3}s\right)\bar{d}\gamma_\mu d + \left(-1+\frac{4}{3}s\right)\bar{s}\gamma_\mu s$$

$$s \equiv \sin^2\theta_W \sim 0.2315$$

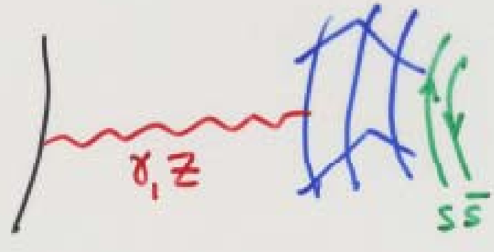

ASYMMETRY

$$A = \frac{d\sigma_L - d\sigma_R}{d\sigma_L + d\sigma_R} \sim \frac{M^{PC} M^{PV}}{(M^{PC})^2}$$

$$= -\frac{G_F Q^2}{4\pi\alpha\sqrt{2}} \frac{\varepsilon G_E^{\gamma} G_E^{Z} + \tau G_M^{\gamma} G_M^{Z} - (1-4s)\epsilon' G_M^{\gamma} G_A^{e}}{\varepsilon G_E^{\gamma 2} + \tau G_M^{\gamma 2}}$$

$$\tau = \frac{Q^2}{4M_p^2}$$

$$\epsilon = \left(1 + 2(1+\tau)\tan^2\frac{\theta}{2}\right)^{-1}$$

$$\epsilon' = \sqrt{\tau(1+\tau)(1-\epsilon^2)}$$

$$G_A^{e} = -\tau_3 \underbrace{G_A}_{1.267} + \Delta_s$$

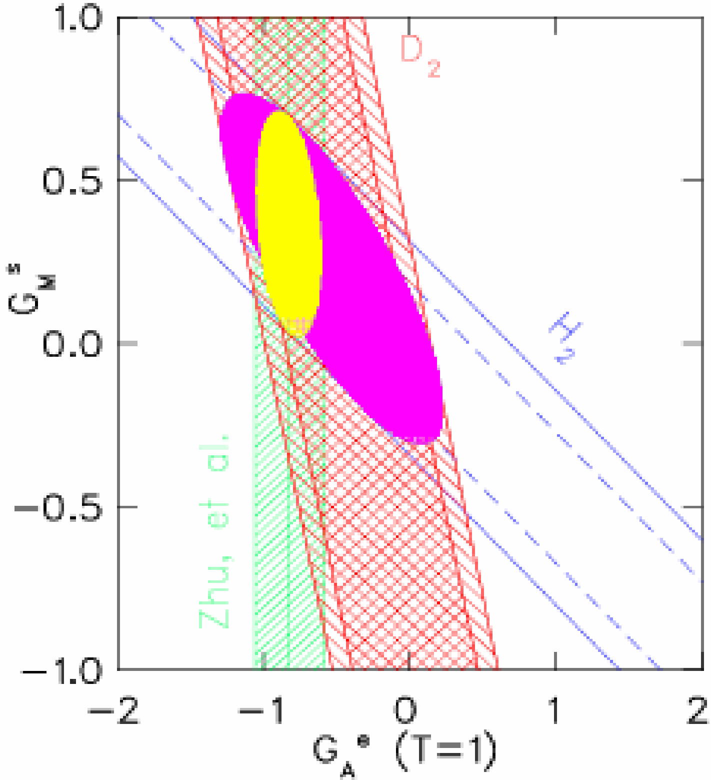

Figure 21: Results from the 200 MeV SAMPLE data, in the space of G_M^s vs. $G_A^{e\,(T=1)}$, along with the theoretically expected value of $G_A^{e\,(T=1)}$, using [18] for the weak radiative corrections. The ellipses correspond to a 1-σ overlap of the two data sets (larger) and the hydrogen data and theory (smaller).

SAMPLE E.J.Beise, Prog.Part.Nucl.Sci, 54, 289 (2005)

BUT μ_s SHOULD BE NEGATIVE!

☆ ASYMMETRIC LONG TERM FLUCTUATION

... PSEUDOSCALAR MESON LOOP

$$\langle K^+ \Lambda^0 \mid T \mid p \rangle \sim \langle \mid \vec{\sigma}\cdot\vec{q} \mid \rangle$$

$p\uparrow$ $(+e)$ $\qquad$ $\Lambda\downarrow$ $(-e/3)$

K^+ $\quad l_z = +1$ $\quad (e/3)$

POSITIVE MAGNETIC MOMENT CONTRIBUTION

BUT... MULTIPLY BY -3

$(\langle \bar{s} | \gamma_\mu | s \rangle)$

⇨ NEGATIVE G_M^S !

IF POSITIVE G_M^S

★ VECTOR MESON LOOPS

CHARGE COUPLING $\gamma_0 \; K_0^*$ SPIN NON-FLIP

POSITIVE !

CURRENT COUPLING $\vec{\gamma} \cdot \vec{K}^*$ SPIN-FLIP

NEGATIVE

★★ VM LOOPS WITH $K^* K \gamma$ VERTEX

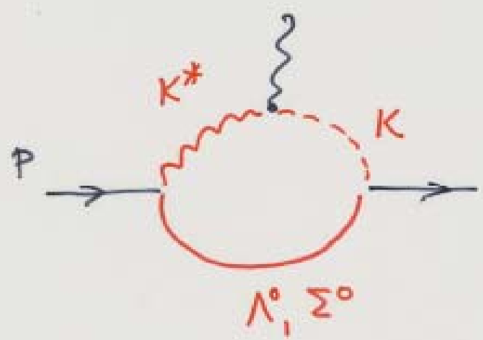

POSITIVE !

Geiger-Isgur

PRD 55, 299 (1997)

Table 3: Theoretical predictions for $\mu_s \equiv G_M^s(Q^2 = 0)$ and r_s^2.

Type of calculation	μ_s (n.m.)	r_s^2 (fm^2)	Reference
Poles	-0.31 ± 0.09	$0.11 \rightarrow 0.22$	(32)
Kaon Loops	$-0.31 \rightarrow -0.40$	$-0.032 \rightarrow -0.027$	(27)
Kaon Loops	-0.026	-0.01	(28)
Kaon Loops	$\lvert\mu_s\rvert = 0.8$		(29)
SU(3) Skyrme (broken)	-0.13	-0.10	(36)
SU(3) Skyrme (symmetric)	-0.33	-0.19	(36)
SU(3) chiral hyperbag	$+0.42$		(37)
SU(3) chiral color dielectric	$-0.20 \rightarrow -0.026$	-0.003 ± 0.002	(44)
SU(3) chiral soliton	-0.45	-0.35	(38)
Poles	-0.24 ± 0.03	0.19 ± 0.03	(33)
Kaon Loops	$-0.125 \rightarrow -0.146$	$-0.022 \rightarrow -0.019$	(30)
NJL soliton	$-0.05 \rightarrow +0.25$	$-0.25 \rightarrow -0.15$	(42)
QCD equalities	-0.75 ± 0.30		(45)
Loops	$+0.035$	-0.04	(31)
Dispersion	$-0.10 \rightarrow -0.14$	$0.21 \rightarrow 0.27$	(35)
Chiral models	$-0.25, -0.09$	0.24	(46)
Poles	0.003	0.002	(34)
SU(3) Skyrme (broken)	$+0.36$		(39)
Lattice (quenched)	-0.36 ± 0.20	$-0.06 \rightarrow -0.16$	(40)
Lattice (chiral)	-0.16 ± 0.18		(41)

D.Beck and R.D.McKeown, Ann Rev Nucl Part Sci **51** 189 (2001)

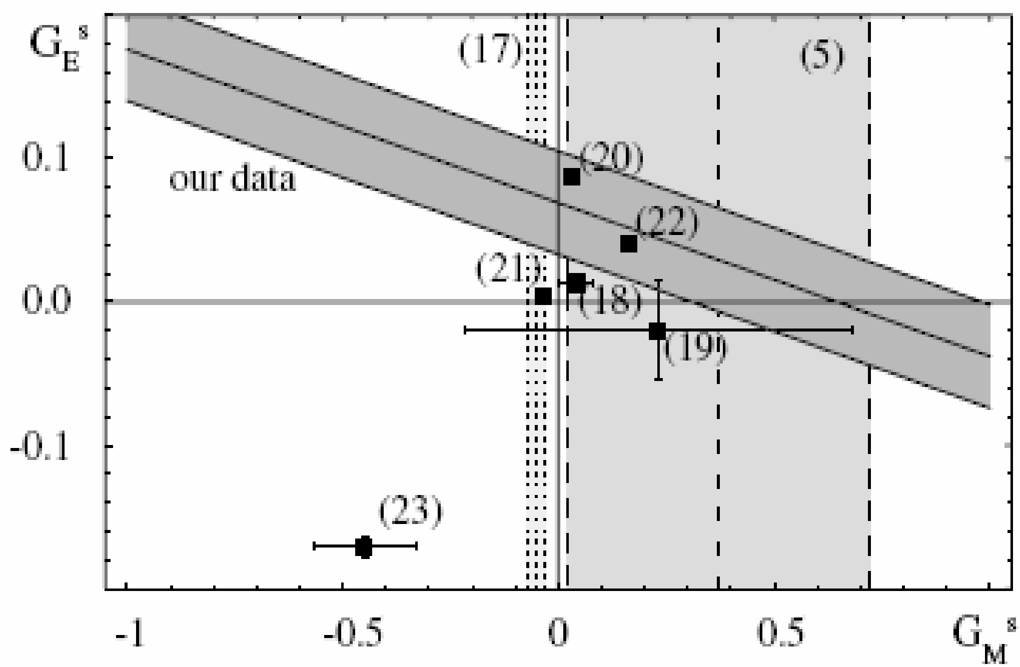

FIG. 3. The solid lines represent our result on $G_E^s + 0.106 G_M^s$ as extracted from our new data presented here. The shaded region represents in all cases the one-σ uncertainty with statistical and systematic and theory error added in quadrature. The dashed lines represent the result on G_M^s from the SAMPLE experiment [5]. The dotted lines represent the result of a recent lattice gauge theory calculation for μ_s [17]. The black squares represent different model calculations, and the numbers denote the references.

A4 F.E.Maas et al, PRL 94, 152001 (2005)

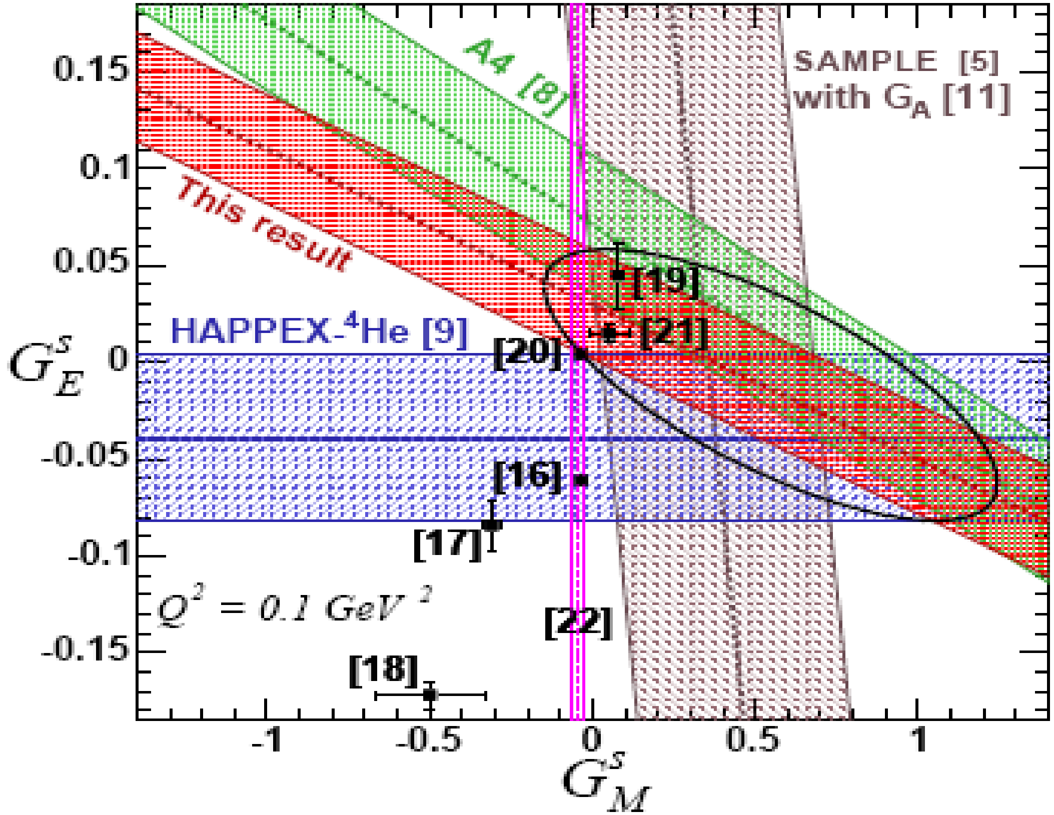

FIG. 3: The four A_{PV} measurements at $Q^2 \sim 0.1\,\mathrm{GeV}^2$ are shown, with shaded bands representing the 1-sigma combined statistical and systematic uncertainty. Also shown is the combined 95% C.L. ellipse from all four measurements. The black squares and narrow vertical band represent various theoretical calculations ([16]-[22]).

HAPPEX K.A.Aniol et al, nucl-ex/0506011

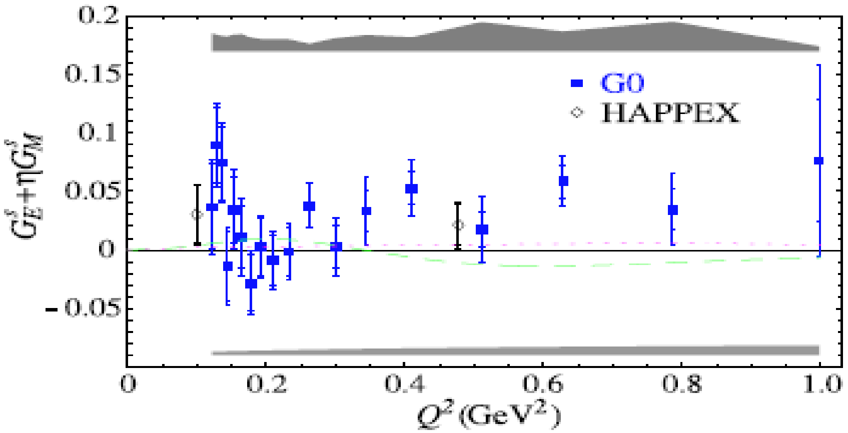

FIG. 2: The combination $G_E^s + \eta G_M^s$ for the present measurement. The gray bands indicate systematic uncertainties (to be added in quadrature); the lines correspond to different electromagnetic nucleon form factor models (see text).

terize our result with a single number, we tested the hypothesis $G_E^s + \eta G_M^s = 0$ by generating randomized data sets with this constraint, distributed according to our statistical and systematic uncertainties (including correlated uncertainties). The fraction of these with χ^2 larger than that of our data set was 11%, so we conclude that the non-strange hypothesis is disfavored with 89% confidence. More important is the Q^2 dependence of the data. The initial rise from zero to about 0.05 is consistent with the finding that $G_M^s(Q^2 = 0.1\ \mathrm{GeV}^2) \sim +0.5$ from the SAMPLE [24], PVA4 [25] and HAPPEX [17] measurements. Because η increases linearly throughout,

G0 D.S.Armstrong et al nucl-ex/0506021

NOT AN OPTIMAL APPROACH

STRANGENESS FLUCTUATIONS OF BARYONS

... MUSOLF & BURKHARDT, Z. PHYS. <u>C41</u> (1994) 433

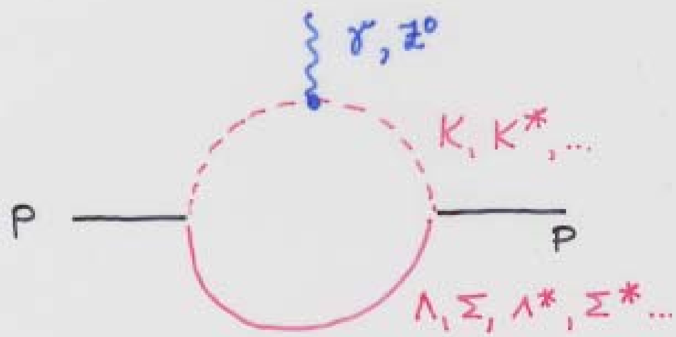

$\int_0^1 dx \; \ldots$

$$\sim \frac{1}{\pi} \quad \frac{g_{K\Lambda N}^2}{4\pi} \quad \frac{m_p^2}{m_p^2 + m_K^2} \quad \sim 1.2$$

0.3 5 0.8

[reduced by cut-offs]

~ LARGE, DIVERGENT LOOP EXPANSION

~ SMALL RESULTS ONLY BY CANCELLATIONS BETWEEN MANY LARGE CONTRIBUTIONS

TABLE I. Intermediate state contributions to the strange magnetic moment μ_s and the electric strangeness radius $\langle r_s^2 \rangle_D$ in the loop model of [19].

	$\langle r_s^2 \rangle_D$ (fm^2)		μ_s	
Λ (GeV)	1.2	2.2	1.2	2.2
$KK\Lambda$	-0.007		-0.237	
$K^*K^*\Lambda$	0.0023	0.030	-0.180	-4.149
$KK^*\Lambda$	0.0207	0.085	0.253	1.023

H.Forkel et al PR C 61, 055206 (2000)

L. Barz et al Nucl Phys A 640, 259 (1998)

A SMALL VALUES APPROACH

STRANGENESS FLUCTUATIONS OF CONSTITUENT QUARKS

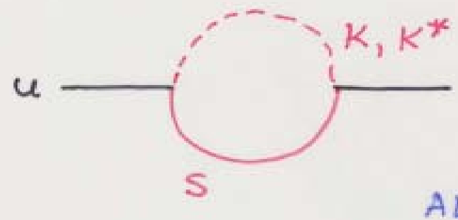

ALL INTERMEDIATE HYPERONS INCLUDED

$$\sim -\frac{1}{\pi}\ \frac{g_{Kus}^2}{4\pi}\ \frac{m_u^2}{m_u^2 + m_K^2} \sim -0.06$$

0.3 0.7 0.3

Ramsey-Musolf & Ito, PRC 55 (1997) 3066

Hannelius, DoR & Glozman,* hep-th/9908393

Geiger & Isgur, PRD55 (1997) 299

* $\mu_s \sim -0.046$

- K,K* loops in the "chiral" quark model

$\mu_s = -\ 0.046$ nm

L. Hannelius & DOR, PRC 62, 045204 (2000)

- QCD Lattice calculation with chiral extrapolation

$\mu_s = -\ 0.046 \pm 0.019$ nm

D.B.Leinweber & al, PRL 94, 212001 (2005)

" tremendous challenge for future experiments"

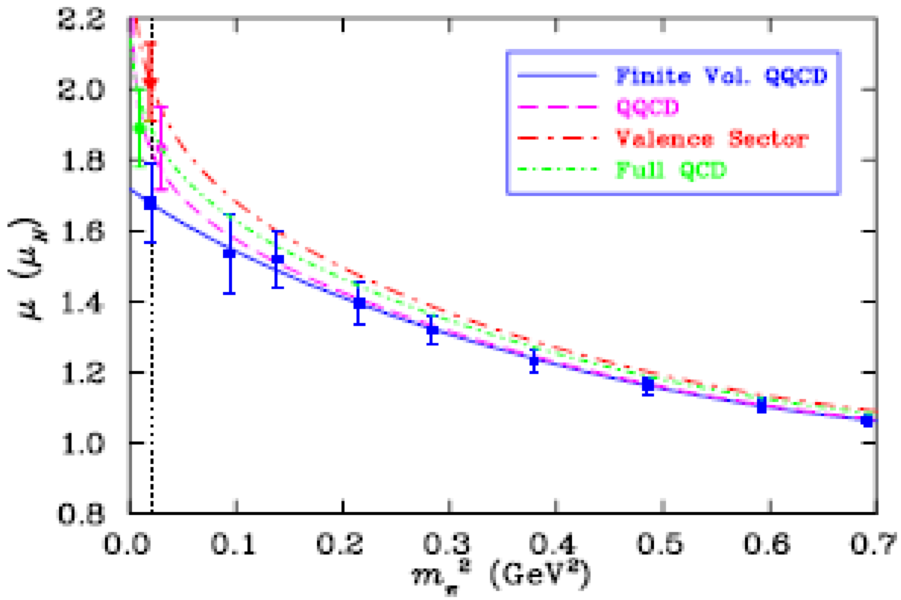

FIG. 4 (color online). The contribution of a single u quark (with unit charge) to the magnetic moment of the proton. Lattice simulation results (square symbols for $m_\pi^2 > 0.05$ GeV) are extrapolated to the physical point (vertical dashed line) in finite-volume QQCD as well as infinite-volume QQCD, valence, and full QCD; see text for details. Extrapolated values at the physical pion mass (vertical dashed line) are offset for clarity.

D. Leinweber et al, PRL 94, 212001 (2005)

APPROXIMATIONS & CORRECTIONS

- Pion mass extrapolation
- Charge symmetric sea
- Two-photon exchange

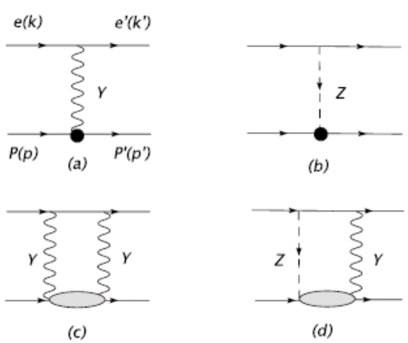

FIG. 1: Diagrams of Born approximation (a, b), two-photon exchange (c) and γZ box (d) for elastic e-p scattering in a Standard Model of electroweak interactions. Corresponding cross-box diagrams are implied.

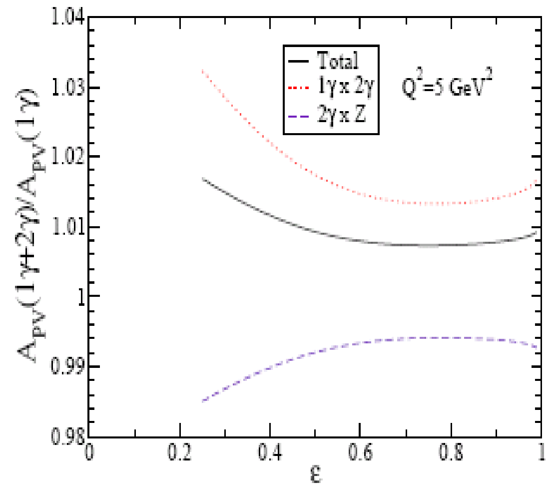

FIG. 2: Two-photon exchange correction to parity-violating asymmetry as a function of ϵ at $Q^2 = 5$ GeV^2. Also shown are separate effects from the parity-conserving $1\gamma \times 2\gamma$-interference and parity-violating $2\gamma \times Z$-interference.

Afanasev and Carlson
PRL 94, 212301 (2005)

uuds$\bar{s}$ CONFIGURATIONS

COLOR 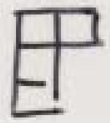 [211]

SPACE 

uuds

GROUND STATE

$\bar{s}$ $L=1$

cf. KAON LOOPS

uuds

$L=1$

s $L=0$

FLAVOR-SPIN

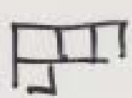

SPIN DEPENDENT HYPERFINE INTERACTION LOWERS ANTISYMMETRIC SPIN STATES

$$\langle S=0 \,|\, \boldsymbol{\sigma}^1 \cdot \boldsymbol{\sigma}^2 \,|\, S=0 \rangle = -3$$
$$\langle S=1 \,|\, \boldsymbol{\sigma}^1 \cdot \boldsymbol{\sigma}^2 \,|\, S=1 \rangle = +1$$

- COLOR MAGNETIC H.F. INTERACTION

$$V = (2\pi / 9\, m^2)\, \alpha_S\, \boldsymbol{\sigma}^1 \cdot \boldsymbol{\sigma}^2\, \delta(r)$$

- FLAVOR-SPIN INTERACTION

$$V_\chi = -\, C_\chi\, \Sigma_{ij}\, \boldsymbol{\lambda}_i \cdot \boldsymbol{\lambda}_j\, \boldsymbol{\sigma}^i \cdot \boldsymbol{\sigma}^j \qquad C_\chi \sim 30 \text{ MeV}$$

$$\langle N \,|\, \Sigma\, \boldsymbol{\sigma}^i \cdot \boldsymbol{\sigma}^j \,|\, N \rangle = +1 - 3 = -2$$
$$\langle N \,|\, \boldsymbol{\Sigma} \boldsymbol{\sigma}^i \cdot \boldsymbol{\sigma}^j \;\; \boldsymbol{\tau}^i \cdot \boldsymbol{\tau}^j \,|\, N \rangle = 1 \cdot 1 + (-3) \cdot (-3) = +10$$

SCHEMATIC FLAVOR-SPIN INTERACTION

$$H = -C \sum_{i<j} \vec{\sigma}^i \cdot \vec{\sigma}^j \; {}_m\lambda_F^i \cdot {}_n\lambda_F^j$$

π + ππ EXCHANGE

SU(3) MATRICES

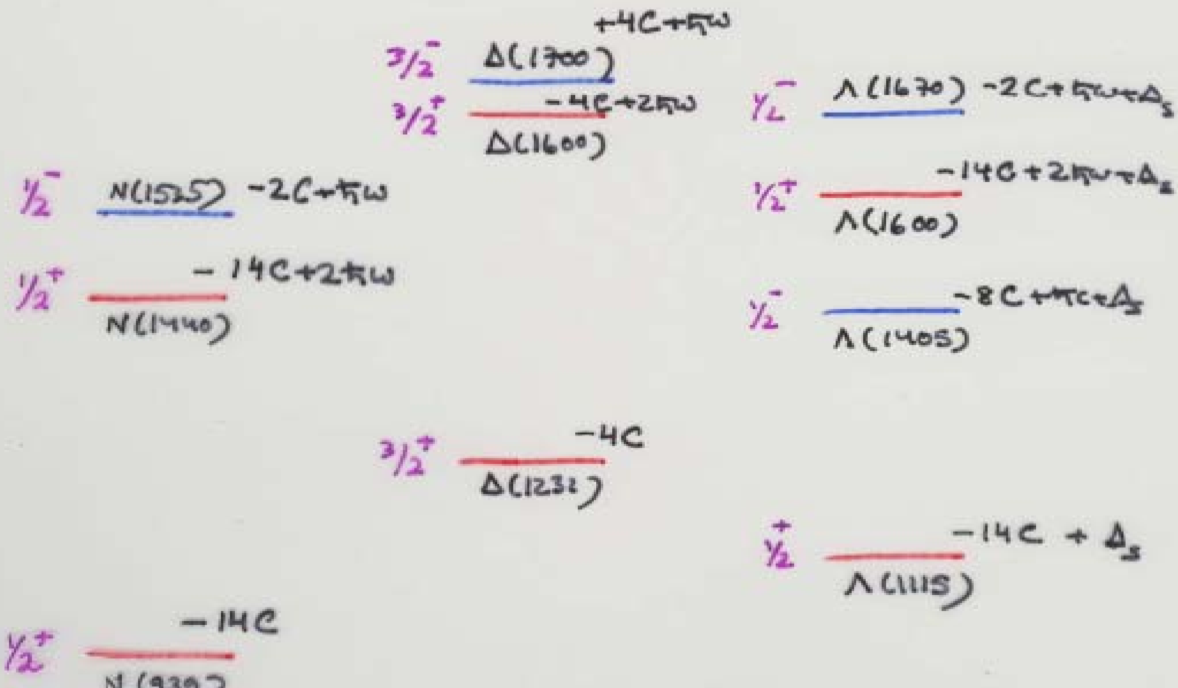

$\Delta_s = m_s - m_u$

TABLE I: Flavor and spin state symmetry configurations of the $uuds$ quark states in the ground state and first orbitally excited P state. The states are ordered from above after increasing matrix elements of the Casimir operator $-\sum_{i<j}\vec{\lambda}_i\cdot\vec{\lambda}_j\vec{\sigma}_i\cdot\vec{\sigma}_j$, where λ_i are the $SU(3)_F$ generators. These matrix elements are listed in the brackets [17].

$uuds$ ground state		$uuds$ $P-$state	
$[31]_{FS}[211]_F[22]_S$	(-16)	$[4]_{FS}[22]_F[22]_S$	(-28)
$[31]_{FS}[211]_F[31]_S$	(-40/3)	$[4]_{FS}[31]_F[31]_S$	(-64/3)
$[31]_{FS}[22]_F[31]_S$	(-28/3)	$[31]_{FS}[211]_F[22]_S$	(-16)
$[31]_{FS}[31]_F[22]_S$	(-8)	$[31]_{FS}[211]_F[31]_S$	(-40/3)
$[31]_{FS}[31]_F[31]_S$	(-16/3)	$[31]_{FS}[22]_F[31]_S$	(-28/3)
$[31]_{FS}[31]_F[4]_S$	(0)	$[31]_{FS}[31]_F[22]_S$	(-8)
$[31]_{FS}[4]_F[31]_S$	(+8/3)	$[4]_{FS}[4]_F[4]_S$	(-8)
		$[22]_{FS}[211]_F[31]_S$	(-16/3)
		$[31]_{FS}[31]_F[31]_S$	(-16/3)
		$[22]_{FS}[22]_F[22]_S$	(4)
		$[211]_{FS}[211]_F[22]_S$	(0)
		$[31]_{FS}[31]_F[4]_S$	(0)
		$[211]_{FS}[211]_F[31]_S$	(8/3)
		$[22]_{FS}[31]_F[31]_S$	(8/3)
		$[31]_{FS}[4]_F[31]_S$	(8/3)
		$[22]_{FS}[22]_F[4]_S$	(4)
		$[211]_{FS}[22]_F[31]_S$	(20/3)
		$[211]_{FS}[211]_F[4]_S$	(8)
		$[211]_{FS}[31]_F[22]_S$	(8)
		$[22]_{FS}[4]_F[22]_S$	(8)
		$[211]_{FS}[31]_F[31]_S$	(32/3)

DEFINITION OF μ_s

- $\boldsymbol{\mu}_s = e\, \Sigma_i\, (\hat{S}_i / 2\, m_s)\ (\, \mathbf{l}_i + \boldsymbol{\sigma}_i\,)$
- $\hat{S}_i = +1\ \ (s)\ ,\quad -1\ \ (\bar{s})$ *strangeness counting operator*
- B.S.Zou & DOR, Phys. Rev. Lett. 95, 072001 (2005)

THE LOWEST ENERGY CONFIGURATIONS

- $\bar{s}$ in the P-state:
  $[31]_{FS}[211]_F\ [22]_S$

$$\mu_s = -(1/3)\,(m_p\,/m_s)\,P_{s\hat{s}}$$

$$\psi = A_{s\bar{s}} \sum_{a,b,c} \sum_{m,s,M,J,j} (1,1/2,m,s|J,j)\,(S,J,M,j|1/2,1/2)\,C^{[1111]}_{[211]a,[31]a} C^{[31]a}_{[F]b,[S]c} [211]_C(a)\,[F](b)\,[S]_M(c)\,\bar{Y}_{1m}\,\bar{\chi}_s \varphi(\{r_i\})\,. \qquad (2)$$

- $\bar{s}$ in the S-state:
  $[4]_{FS}[22]_F\ [22]_S$
  - Lower by ~ 360 MeV

$$\mu_s = +(1/2)\,(m_p\,/m_s)\,P_{s\hat{s}} \sim P_{s\hat{s}}$$

$$\psi = A_{s\bar{s}} \sum_{a,b,c,d,e} \sum_{m,s,M,j} (1,S,m,M|\,J,j)\,(J,1/2,j,s|\,1/2,1/2)\,C^{[1111]}_{[211]a,[31]a} C^{[31]a}_{[31]b,[FS]c} C^{[FS]c}_{[F]d,[S]e} [211]_C(a)\,[31]_{X,m}(b)\,[F](d)\,[S]_M(e)\,\bar{\chi}_s\,\varphi(\{r_i\})\,. \qquad (7)$$

SAMPLE: $\mu_s = 0.37 \pm 0.2 \pm 0.26 \pm 0.07$

General expressions
$\hat{s}$ in P - state

$[31]_{FS}\,[F]_F\,[22]_S$: $\mu_s = -\,(1/3)\,(m_p/m_s)\,P_{s\hat{s}}$

$[31]_{FS}\,[F]_F\,[31]_S$: $\mu_s = -\,(7/6 - 1/2\sigma)\,(m_p/m_s)\,P_{s\hat{s}}$

$[31]_{FS}\,[31]_F\,[4]_S$: $\mu_s = +\ 7/6\,(m_p/m_s)\,P_{s\hat{s}}$

σ average spin z-component for S=1 uuds state

$(\sigma < 1)$

General expressions
$\hat{s}$ in S - state

$[FS]_{FS}[F]_F[22]_S$: $\mu_s = + (1/3 + 2/3\ \ell)\ (m_p/m_s)\ P_{s\hat{s}}$

$[FS]_{FS}[F]_F[31]_S$: $\mu_s = -\ (m_p/m_s)\ P_{s\hat{s}}$, J=0

$[FS]_{FS}[F]_F[31]_S$: $\mu_s = + (1/3)(1 + \ell + \sigma)\ (m_p/m_s)\ P_{s\hat{s}}$,

J=1

$[FS]_{FS}[F]_F[4]_S$: $\mu_s = +(5/6 - 1/3\ \ell)\ (m_p/m_s)\ P_{s\hat{s}}$

ℓ average m_z in L=1 state

($\ell < 1/2$)

Θ^+ quark cluster models

Jaffe-Wilczek: two scalar diquarks [ud], [us] in relative P-state & ŝ in S-state:

$$\mu_s = 1/3\ (m_p / m_s)\ (1 + 2\ m_s / m_{ud} + m_{us}) P_{s\hat{s}} > 0$$

Shuryak-Zahed: scalar + tensor diquark ℓ=1) & ŝ

$$\mu_s = \tfrac{1}{2}\ (m_p / m_s)\ (1 + \ m_s / 3 m_{us})\ P_{s\hat{s}} > 0$$

Karliner-Lipkin: scalar [ud] + [udŝ] triquark in L=1 state:

$$\mu_s = -1/3\ (m_p / m_s)\ \ P_{s\hat{s}} \quad < \ 0$$

5 quark components in $\Delta(1232)$

$\Gamma(\Delta(1232) \rightarrow N\pi) < 50\ \%$ of $\Gamma_{exp} \sim 120$ MeV

Recent examples:

B. Julia-Diaz, DOR & F.Coester PRC 70 (2004):
Covariant quark model that describes $G_E(p)$ in all forms of relativistic kinematics (instant, point & front)
$\Gamma(\Delta(1232) \rightarrow N\pi)$: 40 -45 MeV

T. Melde et al. hep-ph/0406023:
Dynamic quark model for the spectrum, 3 models for the hyperfine interaction (Gluon exch, meson exch, instanton ind. interaction
$\Gamma(\Delta(1232) \rightarrow N\pi)$: 32 -60 MeV

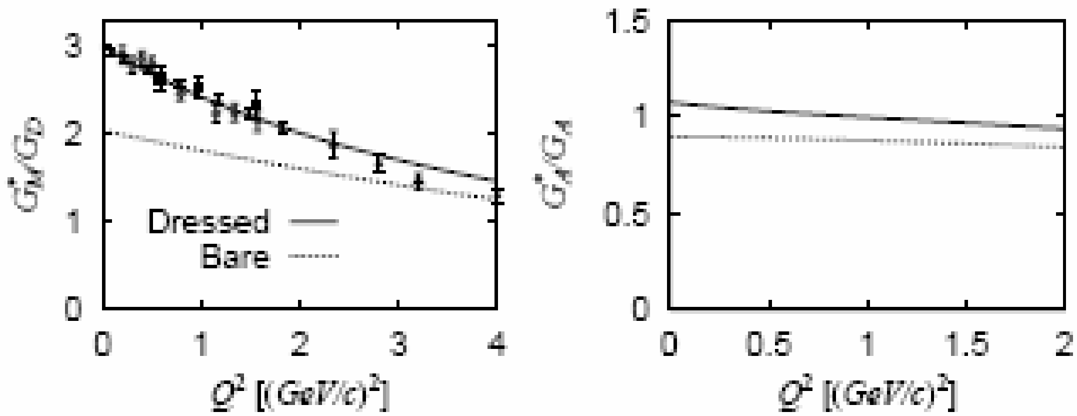

FIG. 9. The N-Δ form factors predicted by model I, left panel: magnetic $M1$ form factors given in Ref. [2], right panel: axial vector form factor. The solid curves are from full calculations. The dotted curves are obtained from turning off the pion cloud effects. $G_D = 1/(1+Q^2/M_V^2)^2$ with $M_V = 0.84$ GeV is the usual proton dipole form factor and $G_A = 1/(1+Q^2/M_A^2)^2$ with $M_A = 1.02$ GeV is the axial nucleon form factor of Ref. [31].

Sato-Uno-Lee PRC 67, 065201 (2003)

$qqqq\bar{q} \longrightarrow qqq + (q\bar{q})$

Q.B Li & DOR, nucl-th/0507008

LOWEST ENERGY $qqqq\bar{q}$ COMPONENT IN Δ

$[4]_{FS}\ [31]_{F}\ [31]_{S}$

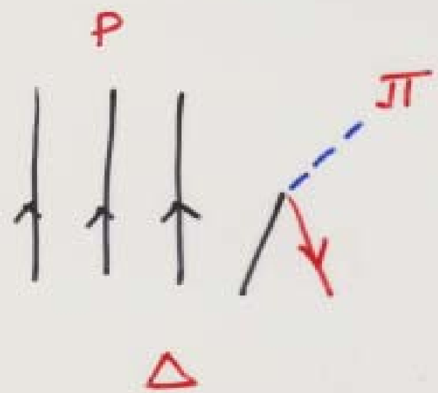

10% $qqqq\bar{q}$ $\Gamma_{calc}(\Delta \rightarrow p\pi)$

INCREASES BY 48%

CONFINEMENT TRIGGERED ANNIHILATION

$$qqqq\bar{q} \longrightarrow qqq + (q\bar{q})$$

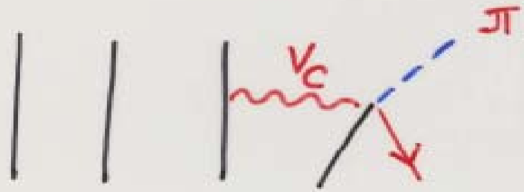

DIRECT ANNIHILATION

$$T = i\sqrt{2}\ \frac{m_q\, g_A^q}{f_D}\ \bar{v}(p_{\bar{q}})\,\gamma_5\, u(p_q)$$

SCALAR CONFINEMENT

$$m_q \longrightarrow m_q + \frac{V_c(r)}{2}$$

10% $qqqq\bar{q}$ $\qquad \Gamma_{calc} \sim (\underbrace{2}_{\substack{\text{OSCILLATOR}\\ \frac{1}{2}Cr^2}} - \underbrace{3}_{\substack{\text{LINEAR}\\ V_c(r) = cr}}) \times \Gamma_{quark\ model}$

Summary

- The strangeness magnetic moment is most likely positive SAMPLE, A4, HAPPEX, G0

- The sŝ component in the proton is probably such that the uuds is in the P state and the ŝ is in the ground state

- uuudđ components in the Δ(1232) is the reason for the systematic underestimate of the decay width in the 3 valence quark model